Weakly incoherent magnetotransport in layered metals

P. D. Grigoriev*
L. D. Landau Institute for Theoretical Physics, Chernogolovka, Russia
(Dated: October 6, 2010)

We investigate electronic conductivity in layered metals in magnetic field in the weakly incoherent limit, when the interlayer transfer integral is smaller than the Landau level broadening due to the impurity potential, but the interlayer electron tunnelling conserves the intralayer momentum. It is shown that the impurity potential has much stronger effect in this regime, than in the quasi-2D metals in the coherent limit. The weakly incoherent regime has several new qualitative features, not found in the previous theoretical approaches. The background interlayer magnetoresistance in this regime monotonically grows with increasing of magnetic field perpendicular to the conducting layers. The effective electron mean free time is considerably shorter than in the coherent regime and decreases with magnetic field. This enhances the role of higher harmonics in the angular magnetoresistance oscillations and increases the Dingle temperature, which damps the magnetic quantum oscillations.

I. INTRODUCTION

The crossover between coherent and incoherent electron transport in the layered metals attracts great attention, both theoretical [1–8] and experimental,[8–14] for its influence on the properties of high-temperature cuprate superconductors, organic metals, heterostructures, and many other layered materials. This crossover can be driven by temperature T, volume impurity concentration n_i, external magnetic field $\mathbf{B} = (B_x, B_y, B_z)$. In magnetic field this crossover in conductivity is very pronounced because it qualitatively changes the magnetoresistance behavior.

The electronic conductivity in magnetic field is widely used to investigate the electronic structure of various metals. In strongly anisotropic quasi-2D layered metals, when the interlayer transfer integral t_z is much smaller than the Fermi energy E_F, the influence of magnetic field on conductivity has many specific features. One has to separate several different regimes of interlayer magnetotransport, depending on the ratios of three energy parameters: the interlayer transfer integral t_z, the inverse mean free time $\Gamma_0 = \hbar/2\tau_0$ due to the impurity scattering, and the Landau level (LL) separation $\hbar\omega_c$, where $\omega_c = eB_z/m^*c$ is the cyclotron frequency.

When the interlayer transfer integral is larger than the Landau level separation, $t_z > \hbar\omega_c$, the 3D electronic dispersion is well defined and given in the tight-binding approximation by

$$\epsilon_{3D}\left(\mathbf{k}\right) \approx \epsilon\left(k_x, k_y\right) - 2t_z \cos(k_z d), \tag{1}$$

where $\epsilon\left(k_x, k_y\right)$ is the in-plane electron dispersion and d is the interlayer spacing. Then the classical magnetoresistance shows Yamaji oscillations,[15, 16] which are used to determine the in-plane Fermi momentum. The magnetic quantum oscillations (MQO) of interlayer conductivity in this case have beats of amplitude,[17] and these beats are shifted with respect to the beats of MQO of magnetization or of the other thermodynamic quantities.[18–20] The slow oscillations also appear in the interlayer conductivity, which can be used to separate relaxation times from different scattering mechanisms.[20, 21]

When the interlayer transfer integral is smaller than the Landau level separation, $t_z < \hbar\omega_c$, the beats of MQO disappear. This limit happens in strong fields in very anisotropic metals. If the interlayer transfer integral is still larger than the LL broadening, $t_z > \Gamma$, the dispersion (1) survives, and the MQO can be described by the "coherent" theory in Refs. [18–24]. Note, that the LL broadening Γ is larger than Γ_0 in strongly anisotropic metals close to a stack of isolated conducting layers [see Eq. (20) below].

In the very anisotropic dirty limit, when the interlayer transfer integral is the smallest parameter, $t_z < \hbar\omega_c, \Gamma$, the traditional 3D approach fails to describe the interlayer magnetoresistance. For example, in this limit, the experimentally observed interlayer magnetoresistance grows with increasing of the out-of-plane magnetic field strength B not only in the maxima, but also in the minima of MQO (see, e.g., Refs. [8–10, 12]). The angular dependence of the background magnetoresistance also has many unusual features in this regime.[8, 12] This change of the magnetoresistance behavior as the magnetic field strength or the impurity concentration increase was called the "coherence-to-incoherence crossover". It has been observed in various compounds and attracted the considerable theoretical attention.[1, 6, 8] The term "weakly incoherent" has been introduced[1] to separate this regime from the coherent 3D limit $t_z > \hbar/\tau$, and from the completely incoherent regime, where

*Electronic address: grigorev@itp.ac.ru

the electron tunnelling to the adjacent layers does not conserve the in-plane electron momentum. The completely incoherent interlayer electron tunnelling happens when it goes via resonance impurities,[2, 7, 8] due to interaction with phonons[3][5] and in some other models.

The theory of weakly incoherent magnetoresistance in Ref. [1] is based on the phenomenological Green function (see Eq. (53) of Ref. [1]), which is equivalent to

$$G_R^0(\boldsymbol{r}_1, \boldsymbol{r}_2, j, \varepsilon) = \sum_{n,k_y} \frac{\Psi^{0*}_{n,k_y,j}(x_2, y_2)\Psi^0_{n,k_y,j}(x_1, y_1)}{\varepsilon - \varepsilon_n - i\Gamma_0}. \tag{2}$$

Here j is the number of conducting layer, related to the z-coordinate as $z = jd$. The Landau level number n and the momentum component k_y form the complete set of quantum numbers of the 2D electrons in magnetic field with free electron dispersion

$$\varepsilon_n = \hbar\omega_c \left(n + 1/2\right). \tag{3}$$

In magnetic field $\boldsymbol{B} = (B_x, 0, B_z)$ (we may choose $B_y = 0$ without loss of generality because the in-plane dispersion is uniform) the electromagnetic potential in the Landau gauge is $\boldsymbol{A} = (zB_y, xB_z - zB_x, 0)$. Then the 2D electron wave functions are

$$\Psi_{n,k_y,j}\left(x, y\right) = \Psi_n\left(x - l_{Hz}^2\left[k_y + jd/l_{Hx}^2\right]\right) e^{ik_y y}, \tag{4}$$

where

$$\Psi_n\left(x\right) = \frac{\exp\left(-x^2/2l_{Hz}^2\right) H_n\left(x/l_{Hz}\right)}{\left(\pi l_{Hz}^2\right)^{1/4} 2^{n/2}\sqrt{n!}}, \tag{5}$$

$H_n\left(x/l_{Hz}\right)$ is the Hermite polynomial and, for brevity, we introduced the notation of magnetic length components $l_{Hx} = \sqrt{\hbar c/eB_x}$ and $l_{Hz} = \sqrt{\hbar c/eB_z}$. In the Green function in Eq. (2) the impurity scattering produces only the imaginary part of the self-energy $i\Gamma_0$, which is independent of the quantum numbers $\{n, k_y, j\}$ and of the magnetic field strength B. This approximation is incorrect in the weakly incoherent regime, as will be shown in Sec. II below.

The Green function in Eq. (2) is not suitable to study the MQO, because the MQO of the electron density of state (DoS) at the Fermi level lead to the similar oscillations of the electron self-energy, which must be taken into account in the theory of MQO.[19, 20, 22–24] For electrons with 3D dispersion, as in Eq. (1), in the Born approximation and after averaging over the impurity configurations, the imaginary part of the self-energy is proportional to the density of states, i.e. it acquires the oscillating energy dependence:

$$\Gamma = \Gamma\left(\varepsilon\right) = \Gamma_0\left[1 + \rho\left(\varepsilon, B\right)/\rho_0\right], \tag{6}$$

where $\rho\left(\varepsilon\right)$ and ρ_0 are the electron DoS with and without magnetic field. The electron Green function

$$G_R^0(\boldsymbol{r}_1, \boldsymbol{r}_2, j, \varepsilon) = \sum_{n,k_y,k_z} \frac{\Psi^{0*}_{n,k_y,j}(x_2, y_2)\Psi^0_{n,k_y,j}(x_1, y_1)e^{ik_z(z_1-z_2)}}{\varepsilon - \varepsilon_{2D}\left(n, k_y\right) + 2t_z\cos(k_z d) - i\Gamma\left(\varepsilon\right)}. \tag{7}$$

with $\Gamma\left(\varepsilon\right)$ from Eq. (6) has been substituted to the Kubo formula in the calculation of MQO of interlayer conductivity σ_{zz} in quasi-2D metals in Refs. [19, 20, 22–24] The completely incoherent hopping mechanism of the interlayer magnetotransport, which does not conserve the in-plane electron momentum during the interlayer hopping, has also been suggested[6] to explain the exponential growth in interlayer magnetoresistance with decreasing temperature. However, all these approaches cannot explain the monotonic increase of magnetoresistance with increasing B in the minima of MQO, observed in β''-(BEDT-TTF)$_2$SF$_5$CH$_2$CF$_2$SO$_3$.[9, 10]

Below we reexamine the approach based on Eqs. (2)-(7), in the weakly incoherent limit $\hbar\omega_c > \Gamma_0 > t_z$. We argue that Eq. (6) does not hold in this limit, and derive the different formula for the Green function. Then we calculate the interlayer conductivity with the new Green function and show that the new result considerably differs from that in the "coherent" theory in Refs. [1, 18–24]. This explains several new qualitative features of MQO and of the angular dependence of interlayer magnetoresistance observed in the weakly incoherent limit.

II. THE MODEL

The electron Hamiltonian in layered compounds with small interlayer coupling consists of the 3 terms

$$\hat{H} = \hat{H}_0 + \hat{H}_t + \hat{H}_I. \tag{8}$$

The first term $\hat{H}_0$ is the 2D free electron Hamiltonian summed over all layers:

$$\hat{H}_0 = \sum_{m,j} \varepsilon_{2D}(m)\, c^+_{m,j} c_{m,j},$$

where $\{m\}$ is the set of quantum numbers of electrons in magnetic field on a 2D conducting layer, $\varepsilon_{2D}(m)$ is the corresponding free electron dispersion given by Eq. (3), and $c^+_m(c_m)$ are the electron creation (annihilation) operators in the state $\{m\}$. The second term in Eq. (8) gives the coherent electron tunnelling between two adjacent layers:

$$\hat{H}_t = 2t_z \int dxdy[\Psi^\dagger_j(x,y)\Psi_{j-1}(x,y) + \Psi^\dagger_{j-1}(x,y)\Psi_j(x,y)], \tag{9}$$

where $\Psi_j(x,y)$ and $\Psi^\dagger_j(x,y)$ are the creation (annihilation) operators of an electron on the layer j at the point (x,y). We call this interlayer tunnelling Hamiltonian "coherent" because it conserves the in-layer coordinate dependence of the electron wave function (in other words, it conserves the in-plane electron momentum) after the interlayer tunnelling. The last term

$$\hat{H}_I = \sum_i V_i(r) \tag{10}$$

is the impurity potential. The impurities are taken to be point-like and randomly distributed on the layers. The impurity distributions on any two adjacent layers are uncorrelated. The potential $V_i(r)$ of any impurity located at point r_i is given by

$$V_i(r) = U\delta^3(r - r_i). \tag{11}$$

In the 3D limit, when the interlayer transfer integral t_z is much larger than the electron level broadening Γ due to the impurity scattering, the impurity potential $\hat{H}_I$ can be considered as the small perturbation for the electrons with dispersion (1). In the Born approximation this gives $\Gamma = \pi n_i U^2 \rho(E_F)$ in agreement with Eq. (6), where n_i is the volume impurity concentration, and $\rho(E_F)$ is the DoS at the Fermi level. This leads to the standard theory of magnetic quantum oscillations in Q2D metals.[17][20] In the opposite limit, $t_z \ll \Gamma, \hbar\omega_c$, the interlayer hopping t_z must be considered as a perturbation for the disordered uncoupled stack of 2D metallic layers, where Eq. (6) is no more valid.[25–31]

The 2D metallic electron system in magnetic field in the point-like impurity potential has been extensively studied.[25–31] The point-like impurity potential leads to the broadening of the Landau levels, which is described by the density of states (DoS) distribution function $D(E)$. Since each Landau level without disorder is strongly degenerate, even weak impurity potential lifts this degeneracy and leads to the considerable broadening of the Landau levels. The electron Green functions acquire a cut instead of the pole as in Eq. (2). In the self-consistent one-site approximation, the Green function is given by

$$G(\boldsymbol{r}_1, \boldsymbol{r}_2, \varepsilon) = \sum_{n,k_y} \Psi^{0*}_{n,k_y}(r_2)\Psi^0_{n,k_y}(r_1) G(\varepsilon, n), \tag{12}$$

where

$$G(E,n) = \frac{E + E_g(1 - c_i) \pm \sqrt{(E - E_1)(E - E_2)}}{2EE_g}, \tag{13}$$

and the DoS $D(E) = (-1/\pi)\,\mathrm{Im}G_R(E)$ on each LL is described by the dome-like function[25]

$$D(E) = \frac{\sqrt{(E - E_1)(E_2 - E)}}{2\pi |E| E_g}, \tag{14}$$

where the electron energy E is counted from the last occupied LL, $E = \varepsilon - \varepsilon_{2D}(n, k_y)$, and

$$E_g = V_0/2\pi l^2_{Hz}.$$

Here $V_0 = U|\psi(z_i)|^2 \approx U/d$, is the 2D analogue of the strength U of the point-like impurity potential:

$$V_i(x,y) = V_0 \delta(x - x_i)\,\delta(y - y_i), \tag{15}$$

and $\psi(z)$ is the out-of-plane electron wave function. The boundaries of the DoS dome in Eq. (14) are

$$E_1 = E_g(\sqrt{c_i} - 1)^2,\ E_2 = E_g(\sqrt{c_i} + 1)^2, \tag{16}$$

where c_i is the ratio of the 2D impurity concentration, $N_i = n_i d$, to the 2D DoS on one LL, $N_{LL} = 1/2\pi l_{Hz}^2$:

$$c_i = N_i/N_{LL} = 2\pi l_{Hz}^2 n_i d. \tag{17}$$

The function in Eq. (14) is normalized to unity, $\int D(E)\, dE = 1$. $D(E)$ converges at the point $E = 0$, because this point lies outside the DoS dome $E_1 < E < E_2$. The LL broadening

$$\Gamma_B \equiv (E_2 - E_1)/2 = 2E_g\sqrt{c_i} \propto \sqrt{B}. \tag{18}$$

The ratio

$$\frac{\Gamma_B}{\Gamma_0} = \frac{2V_0\sqrt{n_i d/2\pi l_{Hz}^2}}{\pi n_i U^2 \rho(E_F)} \approx \frac{2U\sqrt{n_i N_{LL}/d}}{\pi n_i U^2 \rho(E_F)} = \frac{2\sqrt{n_i U^2 \rho(E_F)\,\hbar\omega_c}}{\pi n_i U^2 \rho(E_F)} = \sqrt{\frac{4\hbar\omega_c}{\pi\Gamma_0}} \tag{19}$$

grows as $\sqrt{B}$ in high magnetic field. Eqs. (18),(19) give the correct asymptotic for the LL broadening in strong magnetic field. In weak magnetic field, when $\hbar\omega_c \ll \Gamma_0$, the mean scattering time τ_B related to level broadening as $\Gamma_B = \hbar/2\tau_B$ and entering the Drude formula, does not depend on the value of magnetic field along the conductivity: $\tau_B = \tau_0$.[32] To get the correct asymptotic behavior for Γ_B both in strong magnetic field and at $B = 0$, one can take the simple function

$$\Gamma_B \approx \Gamma_0 \left[(4\hbar\omega_c/\pi\Gamma_0)^2 + 1\right]^{1/4}. \tag{20}$$

More realistic models of the finite-range impurity potential, and more accurate calculation of the DoS, including the many-site corrections, lead only to the small tails of the DoS dome.[26][28][31] The number of electron states in these tails is much less than the number of states in the DoS dome and can be neglected. However, to include these tails into account and to simplify the subsequent calculation, one can take the Lorentzian DoS distribution with the same broadening:

$$D(E) \approx \frac{\Gamma_B}{\pi(E^2 + \Gamma_B^2)} = -\frac{\mathrm{Im}G_R(E)}{\pi}. \tag{21}$$

Combining Eqs. (12), (A1) and (21) we obtain

$$G(\boldsymbol{r}_1, \boldsymbol{r}_2, \varepsilon) = \sum_{n,k_y} \frac{\Psi^{0*}_{n,k_y}(r_2)\Psi^0_{n,k_y}(r_1)}{\varepsilon - \varepsilon_n - i\Gamma_B}, \tag{22}$$

This Green function will be used in the next section to calculate the interlayer conductivity.

III. CALCULATION OF CONDUCTIVITY.

The interlayer conductivity σ_{zz}, associated with the Hamiltonian (9), can be calculated using the Kubo formula and the formalism, developed for the metal-insulator-metal junctions[33] The conductivity is expressed via the electron on the adjacent layers:

$$\sigma_{zz} = \frac{e^2 t_z^2 d}{\hbar L_x L_y}\left\langle \int d^2\boldsymbol{r} d^2\boldsymbol{r}' \int \frac{d\varepsilon}{2\pi} A(\boldsymbol{r}, \boldsymbol{r}', j, \varepsilon) A(\boldsymbol{r}', \boldsymbol{r}, j+1, \varepsilon)\left[-n_F'(\varepsilon)\right]\right\rangle, \tag{23}$$

where the electron spectral functions

$$A(\boldsymbol{r}, \boldsymbol{r}', j, \varepsilon) = i\left[G_A(\boldsymbol{r}, \boldsymbol{r}', j, \varepsilon) - G_R(\boldsymbol{r}, \boldsymbol{r}', j, \varepsilon)\right], \tag{24}$$

and the advanced (retarded) Green's functions $G_{A(R)}(\boldsymbol{r}, \boldsymbol{r}', j, \varepsilon)$ include interaction with impurities. The product of two spectral functions in Eq. (23) rewrites as

$$\begin{aligned} \Pi \equiv A(\boldsymbol{r}, \boldsymbol{r}', j, \varepsilon) A(\boldsymbol{r}', \boldsymbol{r}, j+1, \varepsilon) = G_A(\boldsymbol{r}, \boldsymbol{r}', j, \varepsilon) G_R(\boldsymbol{r}', \boldsymbol{r}, j+1, \varepsilon) + \\ + G_R(\boldsymbol{r}, \boldsymbol{r}', j, \varepsilon) G_A(\boldsymbol{r}', \boldsymbol{r}, j+1, \varepsilon) - 2\mathrm{Re}G_R(\boldsymbol{r}, \boldsymbol{r}', j, \varepsilon) G_R(\boldsymbol{r}', \boldsymbol{r}, j+1, \varepsilon), \end{aligned} \tag{25}$$

In addition to the terms with the product of Green functions $G_A G_R$, the expression for conductivity also contains the term $-\mathrm{Re}G_R G_R$, which becomes important when MQO are considered.[20, 22] Eq. (46) and subsequent formulas in Ref. [1], where this term is omitted, can be applied only when MQO are disregarded. In strong magnetic field especially in the layered metals, on contrary, the MQO are very strong.

The angular brackets in Eq. (23) mean averaging over impurity configurations. Since the impurity distributions on each layer is uncorrelated with other layers, one can perform this averaging separately for each spectral function independently, which gives:

$$\sigma_{zz} = \frac{e^2 t_z^2 d}{\hbar L_x L_y} \int d^2\boldsymbol{r} d^2\boldsymbol{r}' \int \frac{d\varepsilon}{2\pi} \left\langle A(\boldsymbol{r}, \boldsymbol{r}', j, \varepsilon) \right\rangle \left\langle A(\boldsymbol{r}', \boldsymbol{r}, j+1, \varepsilon) \right\rangle \left[-n_F'(\varepsilon) \right]. \tag{26}$$

The averaged Green (or spectral) functions are translational invariant: $\langle G_R(\boldsymbol{r}, \boldsymbol{r}', j, \varepsilon) \rangle = \langle G_R(\boldsymbol{r} - \boldsymbol{r}', j, \varepsilon) \rangle$.

If the magnetic field is tilted by angle θ with respect to the normal to the conducting planes, $B = (B_x, 0, B_z) = (B\sin\theta, 0, B\cos\theta)$, the Green functions on two adjacent layers acquire the phase shift [see Eq. (49) of Ref. [1]]:

$$G_R(\boldsymbol{r}, \boldsymbol{r}', j+1, \varepsilon) = G_R(\boldsymbol{r}, \boldsymbol{r}', j, \varepsilon) \exp\left\{ ie \left[\Lambda(\boldsymbol{r}) - \Lambda(\boldsymbol{r}') \right] / \hbar \right\}, \tag{27}$$

where

$$\Lambda(\boldsymbol{r}) = -yB_x d = -yBd\sin\theta.$$

Substituting Eq. (27) into Eq. (25) we obtain

$$\begin{gathered} \Pi = 2G_A(\boldsymbol{r}, \boldsymbol{r}', j, \varepsilon) G_R(\boldsymbol{r}', \boldsymbol{r}, j, \varepsilon) \cos\left\{ e \left[\Lambda(\boldsymbol{r}) - \Lambda(\boldsymbol{r}') \right] / \hbar \right\} - \\ -2\mathrm{Re}\left[G_R(\boldsymbol{r}, \boldsymbol{r}', j, \varepsilon) G_R(\boldsymbol{r}', \boldsymbol{r}, j, \varepsilon) \exp\left\{ -ie \left[\Lambda(\boldsymbol{r}) - \Lambda(\boldsymbol{r}') \right] / \hbar \right\} \right]. \end{gathered} \tag{28}$$

and

$$\begin{aligned} \sigma_{zz} \;=\; & \frac{2e^2 t_z^2 d}{\hbar} \int d^2\boldsymbol{r} \int \frac{d\varepsilon}{2\pi} \left[-n_F'(\varepsilon) \right] \times \\ & \times \left\{ \left| \langle G_R(\boldsymbol{r}, \varepsilon) \rangle \right|^2 \cos\left(\frac{eByd}{\hbar} \sin\theta \right) \right. \\ & \left. - \mathrm{Re}\left[\langle G_R(\boldsymbol{r}, \varepsilon) \rangle^2 \exp\left(\frac{ieByd}{\hbar} \sin\theta \right) \right] \right\}. \end{aligned} \tag{29}$$

The term in the third line of Eq. (29) is absent in Eq. (50) of Ref. [1].

In the magnetic field perpendicular to the conducting layers

$$\sigma_{zz} = \frac{2e^2 t_z^2 d}{\hbar} \int d^2\boldsymbol{r} \int \frac{d\varepsilon}{2\pi} \left[\left| \langle G_R(\boldsymbol{r}, \varepsilon) \rangle \right|^2 - \mathrm{Re}\left\langle G_R(\boldsymbol{r}, \varepsilon) \right\rangle^2 \right] \left[-n_F'(\varepsilon) \right]. \tag{30}$$

The integration over $\boldsymbol{r}$ for the Green function of the form (12) is very simple and gives

$$\sigma_{zz} = \frac{2e^2 t_z^2 d\, N_{LL}}{\hbar} \int \frac{d\varepsilon}{2\pi} \left[-n_F'(\varepsilon) \right] \sum_n \left[\left| \langle G_R(\varepsilon, n) \rangle \right|^2 - \mathrm{Re}\left\langle G_R(\varepsilon, n) \right\rangle^2 \right]. \tag{31}$$

With the approximate Green function, given by Eq. (22), Eq. (31) becomes

$$\sigma_{zz} = \frac{2e^2 t_z^2 d\, N_{LL}}{\hbar} \int \frac{d\varepsilon}{2\pi} \sum_n \frac{\left[-n_F'(\varepsilon) \right] 2\Gamma_B^2}{\left[\left(\varepsilon - \varepsilon_n \right)^2 + \Gamma_B^2 \right]^2}. \tag{32}$$

The sum and integral in Eq. (32) is calculated in a standard way, transforming the sum over LL into the harmonic sum by applying the Poisson summation formula:[34]

$$\sum_{n=n_0}^{\infty} f(n) = \sum_{k=-\infty}^{\infty} \int_a^{\infty} e^{2\pi i k n} f(n)\, dn \tag{33}$$

where $a \in (n_0 - 1; n_0)$. Then, performing the integrations, we obtain

$$\sigma_{zz} = \sigma_0(B) \sum_{k=-\infty}^{\infty} (-1)^k \exp\left[\frac{2\pi \left(ik\mu - |k| \Gamma_B \right)}{\hbar\omega_c} \right] \frac{2k\pi^2 T/\hbar\omega_c}{\sinh\left(2k\pi^2 T/\hbar\omega_c \right)} \left[1 + \frac{2\pi |k| \Gamma_B}{\hbar\omega_c} \right]. \tag{34}$$

where

$$\sigma_0(B) = \frac{e^2 t_z^2 \nu_F d}{\hbar \Gamma_B}, \tag{35}$$

$\nu_F = N_{LL}/\hbar\omega_c$ is the DoS at the Fermi level in the absence of magnetic field. Eq. (34) would coincide with Eqs. (17)-(21) of Ref. [22] if Γ_0 and Γ_ε in these equations are replaced by Γ_B. Note, that the nonoscillating part of conductivity $\sigma_0(B)$ is now a function of magnetic field, because $\Gamma_B \propto \sqrt{B}$ in strong magnetic field. This observation contradicts the previous theoretical results[1][22][23], also developed for the almost 2D case, because in these papers the LL width Γ_B was incorrectly taken to have no monotonic dependence on magnetic field, $\Gamma_B = \Gamma_0 + \tilde{\Gamma}$, where $\tilde{\Gamma}$ rapidly oscillates around zero.

Let us now compare how strongly our result differs from the previous results [see, e.g. Eqs. (17-21) of Ref. [22]]. In Fig. 1 we plot the MQO of resistivity $R_{zz}(B) = 1/\sigma_{zz}$, calculated using Eq. (34) with Γ_B given by Eq. (20) [solid blue line] and with $\Gamma_B = \Gamma_0$ [dashed red line]. The difference is evident: the interlayer magnetoresistance shows monotonic growth and weaker oscillating amplitude with increasing magnetic field, than in the old result.

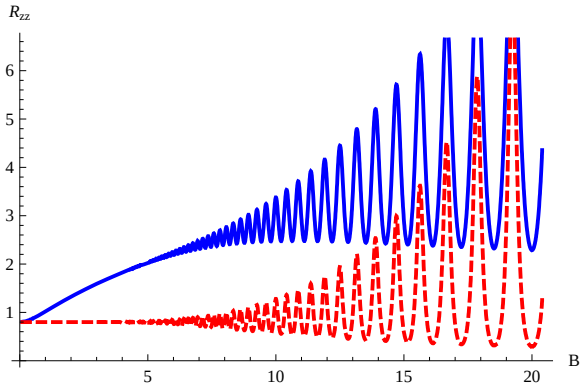

FIG. 1: The MQO of resistivity $R_{zz}(B) = 1/\sigma_{zz}$, calculated using Eq. (34) with Γ_B given by Eq. (20) [solid blue line] and with $\Gamma_B = \Gamma_0$ [dashed red line].

In tilted magnetic field the calculation of Eq. (29) performed in Ref. [1] can be applied with the new magnetic-field-dependent value Γ_B instead of Γ_0, which gives [compare to Eq. (1) of Ref. [1]]

$$\sigma_{zz} = \sigma_0(B) \left\{ [J_0(\kappa)]^2 + 2 \sum_{\nu=1}^{\infty} \frac{[J_\nu(\kappa)]^2}{1 + (\nu\omega_c\tau_B)} \right\}, \tag{36}$$

where $\kappa \equiv k_F d \tan\theta$ and

$$\tau_B = \hbar/2\Gamma_B = \tau_0(\Gamma_0/\Gamma_B). \tag{37}$$

There are two differences between this formula and Eq. (1) of Ref. [1]. First, the higher harmonics in AMRO are weaker damped in Eq. (36) because of smaller value of $\tau_B \propto 1/\sqrt{B}$. Second, as we noted before, the background conductivity $\sigma_0(B)$, given by Eq. (35), decreases as $1/\sqrt{B}$ in strong field.

The higher harmonic in Eq. (36) play considerable role in AMRO. To illustrate this, in Figs. 2,3 we plot the angular dependence of conductivity $\sigma_{zz}(\theta)$ given by Eq. (36) with $\tau_B = \hbar/2\Gamma_B = \tau_0(\Gamma_0/\Gamma_B)$ and $\tau_B = \tau_0$. For simplicity, we take the axially symmetric case, i.e. the symmetric in plane electron dispersion. One can see from Figs. 2,3 that in the minima of conductivity, i.e. at the Yamaji angles, the replacement $\tau_0 \to \tau_B$ is very important. The predicted value of conductivity at the Yamaji angles with τ_B given by Eq. (37) is much larger than with $\tau_B = \tau_0$. This difference increases with increasing of magnetic field. The positions of the conductivity minima, i.e. the Yamaji angles, also slightly shift after the replacement $\tau_0 \to \tau_B$ in Eq. (36) [see Figs. 2,3]. For the first Yamaji angle at $B = 5T$ (see Fig. 2) this shift $\Delta\theta_{Yam} \approx 1.7^\circ$.

IV. DISCUSSION

Let us formulate the main difference of the present approach to the calculation of interlayer conductivity in the weakly incoherent regime compared to the previous methods, developed in Refs. [19][22][20][23][24] to calculate the MQO of conductivity. In these papers the impurity potential is considered as a small perturbation on the background of a free electron gas with well-defined 3D electron dispersion given by Eq. (1). Hence, the impurity scattering was taken into account only by the

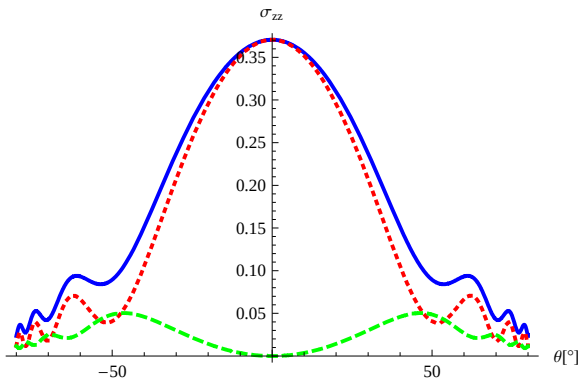

FIG. 2: The angular dependence of conductivity σ_{zz}, calculated using Eq. (36) with τ_B given by Eq. (37) [solid blue line] and with $\tau_B = \tau_0$ [dotted red line]. The dashed green line gives the difference between these two curves. The parameters for this plot are $k_F d = 2,\ m^* = 2m_e,\ B = 5T,\ \Gamma_0 = 1K$.

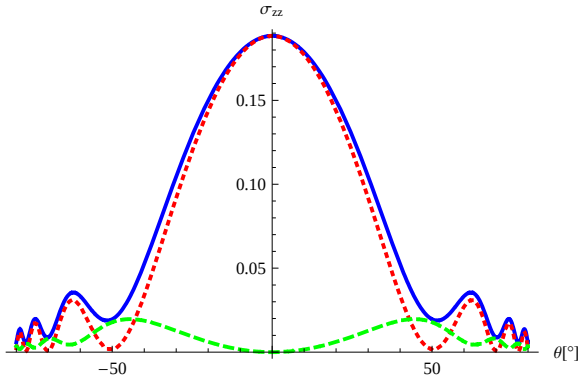

FIG. 3: The angular dependence of conductivity σ_{zz}, calculated using Eq. (36) with τ_B given by Eq. (37) [solid blue line] and with $\tau_B = \tau_0$ [dotted red line]. The dashed green line gives the difference between these two curves. The parameters for this plot are the same as in Fig. 2 besides the larger value of magnetic field $B = 20T$. One can see that in the minima of conductivity, i.e. at the Yamaji angles, the difference is very strong. The predicted value of conductivity at the Yamaji angles with τ_B given by Eq. (37) is much larger than with $\tau_B = \tau_0$.

imaginary part of the electron self-energy given by Eq. (6). Even less accurately the impurities are treated in Ref. [1], where the constant electron mean-free time has been used to include the interaction with impurities. This is correct only in the coherent limit, when the interlayer transfer integral is much larger than the LL broadening, and the electrons, moving in a 3D metal, are scattered by impurities. In the weakly incoherent regime, when $t_z < \Gamma$, this is incorrect, because for a 2D electron system in magnetic field the impurity potential has much stronger effect than in 3D. Simply, in a 3D electron system the electrons after scattering by an impurity move away in the interlayer direction and never return to this impurity. Therefore, this impurity only leads to the single scattering of this electron into some other state, which is well described by the constant electron mean-free time τ_0, or equivalently, by the constant imaginary part Γ_0 of the electron self-energy. In 2D electron system in magnetic field, the electrons after scattering return to the same impurity after the cyclotron period. Therefore, the impurity has permanent influence on the electron state, considerably shifting the electron energy and modifying the electron states. Hence, in the weakly incoherent regime, when $t_z < \Gamma$, the interlayer hopping term (9) in the Hamiltonian (8), rather the impurity potential (10), must be considered as a small perturbation. Therefore, to calculate the interlayer conductivity, we start from the stack of isolated 2D disordered conducting layers in magnetic field, where the effect of impurity potential is considered much more accurately, at least in the self-consistent one-site approximation. Then we substitute the obtained electron Green functions to the Kubo formula for the tunnelling conductivity between adjacent conducting layers. The effect of impurities in the final results turned out to be much stronger than in the previous approaches. Phenomenologically, this difference can be taken into account by the replacement of the initial level broadening Γ_0 by the new value given by Eq. (6).

One can also obtain Eq. (22) with the new value of Γ given by Eq. (20) using different arguments. The physical origin of large DoS broadening in Eq. (14) is not the finite lifetime τ of electron states, with is mathematically described by the imaginary part of the self-energy $\mathrm{Im}\Sigma = \Gamma_0 = \hbar/2\tau$, as in the 3D limit. On the 2D layers the LL broadening comes from the energy shift of each electron state, which is described by the state-dependent real part of the electron self-energy $\mathrm{Re}\Sigma$. The averaging of the electron Green function in Eq. (2) over the impurity configurations is independent on each conducting layer,

since the impurity distribution is assumed to be uncorrelated. Then, the coordinate part of the Green function remains of the form (2) with the bare electron wave functions in numerator [see Eq. (12) and Appendix], but the denominator acquires the real part of electron self energy, which is distributed with the DoS function $D\left(E\right)$:

$$\left\langle G_R^0(\boldsymbol{r}_1,\boldsymbol{r}_2,j,\varepsilon)\right\rangle = \int dE\, D\left(E\right) \sum_{n,k_y} \frac{\Psi^{0*}_{n,k_y,j}(x_2,y_2)\Psi^{0}_{n,k_y,j}(x_1,y_1)}{\varepsilon - E - \hbar\omega_c\left(n+1/2\right) - i\Gamma_0}.$$

The triangular brackets indicate averaging over impurity configurations. Substituting the approximate Lorentzian DoS distribution, given by Eq. (21), one can easily perform the integration over E and obtain

$$\left\langle G_R^0(\boldsymbol{r}_1,\boldsymbol{r}_2,j,\varepsilon)\right\rangle \approx \sum_{n,k_y} \frac{\Psi^{0*}_{n,k_y,j}(x_2,y_2)\Psi^{0}_{n,k_y,j}(x_1,y_1)}{\varepsilon - \hbar\omega_c\left(n+1/2\right) - i\left(\Gamma_0+\Gamma_B\right)}. \tag{38}$$

This Green function differs from Eq. (2) by the increase of the imaginary self-energy part: $\Gamma_0 \to \Gamma_0 + \Gamma_B$ with Γ_B given by Eq. (18). This is almost equivalent to Eq. (22) with Γ_B given by Eq. (20).

Unfortunately, the proposed analysis considers only the limiting case $\Gamma_B \gg t_z$, when Γ_B is given by Eqs. (18) or (20), but it is not accurate for the intermediate case $\Gamma_B \sim t_z$, where the crossover from the coherent to the weakly incoherent regime takes place. The phenomenological formula (20) gives only a qualitative dependence $\Gamma_B\left(B_z\right)$ in this region. The crossover from the coherent to the weakly incoherent regime may be driven by the disorder (impurity concentration) or by magnetic field B_z. The latter happens, because with the increase of magnetic field the effective LL broadening Γ_B also increases [see Eq. (18)] and at some crossover field $B_c \sim t_z^2 m_e^* c/\Gamma_0 e\hbar$ it becomes greater than the interlayer transfer integral t_z. To calculate the exact value B_c of the crossover field and to describe the behavior of interlayer conductivity in this region one needs to calculate the electron Green function in layered metals with impurities and magnetic field in the crossover region $\Gamma_B \sim t_z$. This is an interesting and still open problem.

Above, we have not studied the MQO in the tilted magnetic field. The second term in the curly brackets in Eq. (29) does not contribute to the background magnetoresistance, but it affects the MQO. This term amplifies the MQO and modifies the angular dependence of the MQO amplitude. This modification is a fine effect which is harder to measure. The angular dependence of MQO amplitude is also affected by the Zeeman splitting and possible magnetic ordering.

If the normalized point-like impurity concentration $c_i < 1$, the $N_{LL} - N_i$ electron states on each LL left degenerate, and besides the DoS dome the sharp $\delta\left(E\right)$ term in the DoS survives.[27] However, as has been shown in Ref. [30], the numerous weak impurities and the impurities, situated far from the conducting layers, are important for the lifting of the LL degeneracy in all layered materials. For achievable magnetic field even in the pulsed magnets $B < 100T$, $l_{Hz} > 25\mathring{A}$. Therefore, the typical normalized impurity concentration is greater than unity, $c_i > 1$, and one can use the one-maximum DoS distribution as in Eq. (14).

Above we have shown that the weakly incoherent regime strongly differs from the coherent limit. It also differs from the completely incoherent limit, where the new mechanisms of the interlayer electron transport, including the electron interlayer transport via resonance impurities[2, 7, 8] and the hopping conductivity between completely localized states[6], play important role. One difference of the weakly incoherent regime from the completely incoherent one is that the angular magnetoresistance oscillations (AMRO) are not damped, being of the same amplitude as in the coherent regime. Only higher harmonics in AMRO increase, making AMRO maxima less pronounced. The second difference is that the temperature dependence of conductivity in the weakly incoherent regime is the same, as in the coherent limit (usually, metallic), while the temperature dependence of the hopping conductivity[6] is exponential. Therefore, the weakly incoherent regime of interlayer magnetotransport is a separate regime, which should be distinguished from the coherent and completely incoherent limits.

V. SUMMARY

We reexamine theoretically the conducting properties of layered metals in the "weakly incoherent" regime, when the interlayer transfer integral t_z is much less than the Landau level broadening Γ_B due to the interaction with impurities. The magnetic quantum oscillations and the angular dependence of interlayer conductivity in this regime are calculated. We obtain that both these effects in the weakly incoherent limit considerably differ from the coherent regime. This contradicts the previous theoretical results.[1][22] The background interlayer conductivity σ_{zz} decreases with the increase of magnetic field B_z according to Eq. (35) with Γ_B approximately given by Eq. (20), while in the coherent limit it remains constant (see Fig. 1 for illustration). The Dingle temperature of MQO also increases with magnetic field $\propto \Gamma_B$. Meantime, in the weakly incoherent regime the angular oscillations of background magnetoresistance are not damped as in the completely incoherent mechanisms of the interlayer electron transport, considered, e.g., in Ref. [2],[6],[8]. On contrary, the damping of higher harmonics in the angular magnetoresistance oscillations is weaker than in the coherent regime [see Eqs. (36),(37)]. This leads to the different picture of AMRO (see Figs. 2,3). Phenomenologically, the differences between the coherent and

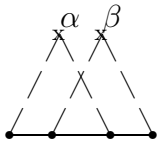

FIG. 4: The first diagram for the electron self-energy with the intersection of the impurity lines.

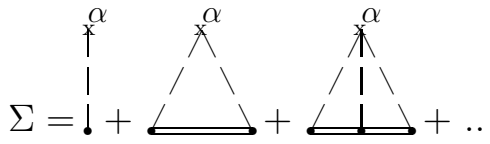

FIG. 5: The set of diagrams for the irreducible self-energy, corresponding to the self-consistent one-site approximation. The double solid line symbolizes the exact electron Green's function.

weakly incoherent regimes can be taken into account by the replacement of the electron mean free time τ_0 by the new value $\tau_B \approx \tau_0 / \left[\left(8\omega_c \tau_0 / \pi \right)^2 + 1 \right]^{1/4}$ in all formulas for MQO and for the angular oscillations of interlayer conductivity.

VI. ACKNOWLEDGEMENT

The work was supported by GK P1419 of the FCP program "Nauchnye i Nauchno-Pedagogicheskie Kadry Rossii", by RFBR and by the grant of the President of Russia MK-2320.2009.2.

Appendix A: The in-plane electron Green function in the impurity potential

Consider the noninteracting 2D electron gas in the potential of randomly distributed point-like impurity, as given in Eq. (15). The peculiarity of the two-dimensional electron gas in strong magnetic field in the presence of impurities is that the Born approximation of the scattering amplitude on each impurity is insufficient to describe the system. Physically, this means that an electron scatters many times by one impurity, because in magnetic field the electrons periodically return to the same point after passing along the cyclotron orbit. In the 3D case the diagram in Fig. 4 with the intersections of impurity lines is small by the parameter n_i/n_e, where n_i and n_e are the volume impurity and electron concentrations. In 2D case in magnetic field there is no general proof that the diagrams with intersections of impurity lines are small. However, the calculations of the DoS in Refs. [26, 28, 31] show that these diagrams only lead to the small tails of the DoS. Therefore, in the our subsequent analysis we keep only the diagrams without intersections of impurity lines.

Now we proof by the method of mathematical induction, that, if one neglects the diagrams with the intersection of impurity lines, the electron Green function, averaged over impurity configurations, has the form of Eq. (12) with

$$G\left(\varepsilon, n\right) = 1/\left[\varepsilon - \varepsilon_n - \Sigma_n\left(\varepsilon\right)\right]. \tag{A1}$$

The energy ε_n of the n-th LL is given by Eq. (3), and the electron wave functions $\Psi^0_{n,k_y}(r)$ by Eq. (4). The self energy part $\Sigma_n\left(\varepsilon\right)$ for the n-th LL must be determined self-consistently and is given by the set of diagrams, shown in Fig. 5. In the self-consistent one-site approximation the self-energy part is

$$\Sigma_n\left(\varepsilon\right) = \frac{E - E_g\left(1 - c_i\right)}{2} \mp \frac{\sqrt{\left(E - E_1\right)\left(E_2 - E\right)}}{2}.$$

The restriction given by Eq. (12) is nontrivial because $G\left(\varepsilon, n\right)$ does not depend on k_y.

Without impurities, i.e. in the zeroth order of mathematical induction, Eq. (12) holds by definition. Assume, it holds for an arbitrary number N of impurities in the electron Green function $G_N(\boldsymbol{r}_1, \boldsymbol{r}_2, \varepsilon)$. When we add one more impurity center, the Green function $G_{N+1}(\boldsymbol{r}_1, \boldsymbol{r}_2, \varepsilon)$ is given by

$$G_{N+1}(\boldsymbol{r}_1, \boldsymbol{r}_2, \varepsilon) = \int dr_\alpha G_N(\boldsymbol{r}_1, \boldsymbol{r}_\alpha, \varepsilon) G_N(\boldsymbol{r}_\alpha, \boldsymbol{r}_2, \varepsilon) \Sigma\left(\varepsilon, \boldsymbol{r}_\alpha\right), \tag{A2}$$

where $\Sigma(\varepsilon)$ is given by the set of diagrams in Fig. 5 with the double-line standing for $G_N(\boldsymbol{r}_\alpha, \boldsymbol{r}_\alpha, \varepsilon)$. Performing the integration over k_y in Eq. (12), we find

$$G_N(\boldsymbol{r}_\alpha, \boldsymbol{r}_\alpha, \varepsilon) = \sum_n \frac{N_{LL}}{\varepsilon - \varepsilon_n - \Sigma_{N,n}(\varepsilon)}.$$

Therefore, $\Sigma(\varepsilon, \boldsymbol{r}_\alpha) = \Sigma(\varepsilon)$, and substituting Eq. (12) into Eq. (A2) and integrating over $\boldsymbol{r}_\alpha$, we obtain

$$\begin{aligned} G_{N+1}(\boldsymbol{r}_1, \boldsymbol{r}_2, \varepsilon) &= \sum_{n,k_y} \frac{\Psi^{0*}_{n,k_y}(r_2)\Psi^0_{n,k_y}(r_1)}{\varepsilon - \varepsilon_n - \Sigma_{N,n}(\varepsilon)} + c_i \int dr_\alpha \sum_{n,k_y} \frac{\Psi^{0*}_{n,k_y}(r_\alpha)\Psi^0_{n,k_y}(r_1)}{\varepsilon - \varepsilon_n - \Sigma_{N,n}(\varepsilon)} \sum_{n',k'_y} \frac{\Psi^{0*}_{n',k'_y}(r_2)\Psi^0_{n',k'_y}(r_\alpha)}{\varepsilon - \varepsilon_{n'} - \Sigma_{N,n'}(\varepsilon)} \Sigma(\varepsilon) + .. \\ &= \sum_{n,k_y} \frac{\Psi^{0*}_{n,k_y}(r_2)\Psi^0_{n,k_y}(r_1)}{\varepsilon - \varepsilon_n - \Sigma_{N,n}(\varepsilon)} \sum_{j=0}^{\infty} \left(\frac{c_i \Sigma(\varepsilon)}{\varepsilon - \varepsilon_n - \Sigma_{N,n}(\varepsilon)} \right)^j = \sum_{n,k_y} \frac{\Psi^{0*}_{n,k_y}(r_2)\Psi^0_{n,k_y}(r_1)}{\varepsilon - \varepsilon_n - \Sigma_{N+1,n}(\varepsilon)}, \end{aligned} \tag{A3}$$

where

$$\Sigma_{N+1,n}(\varepsilon) = \Sigma_{N,n}(\varepsilon) + c_i \Sigma(\varepsilon).$$

Eq. (A3) has the form (12), which proves our statement.

[1] P. Moses and R.H. McKenzie, Phys. Rev. B **60**, 7998 (1999).
[2] A. A. Abrikosov, Physica C 317-318, 154 (1999).
[3] Urban Lundin and Ross H. McKenzie, Phys. Rev. B **68**, 081101(R) (2003).
[4] T. Osada, K. Kabayashi and E. Ohmichi, Synth. Met. **135-136**, 653 (2003).
[5] A. F. Ho and A. J. Schofield, Phys. Rev. B 71, 045101 (2005).
[6] V. M. Gvozdikov,Phys. Rev. B **76**, 235125 (2007).
[7] D. B. Gutman and D. L. Maslov, Phys. Rev. Lett. **99**, 196602 (2007) ; Phys. Rev. B **77**, 035115 (2008).
[8] M. V. Kartsovnik, P. D. Grigoriev, W. Biberacher, and N. D. Kushch, Phys. Rev. B **79**, 165120 (2009).
[9] F. Zuo, X. Su, P. Zhang, J. S. Brooks, J. Wosnitza, J. A. Schlueter, Jack M. Williams, P. G. Nixon, R. W. Winter, and G. L. Gard, Phys. Rev. B **60**, 6296 (1999).
[10] J.Wosnitza, J. Hagel, J. S. Qualls, J. S. Brooks, E. Balthes, D. Schweitzer, J. A. Schlueter, U. Geiser, J. Mohtasham, R. W. Winter, et al., Phys. Rev. B 65, 180506(R) (2002).
[11] T. Valla, P. D. Johnson, Z. Yusof, B.Wells, Q. Li, S. M. Loureiro, R. J. Cava, M. Mikami, Y. Mori, M. Yoshimura, and T. Sasaki, Nature London **417**, 627 (2002).
[12] M.V. Kartsovnik, D. Andres, S.V. Simonov, W. Biberacher, I. Sheikin, N. D. Kushch, and H. Müller, Phys. Rev. Lett. **96**, 166601 (2006).
[13] J. G. Analytis, A. Ardavan, S. J. Blundell, R. L. Owen, E. F. Garman, C. Jeynes, and B. J. Powell, Phys. Rev. Lett. 96,177002 (2006).
[14] V. N. Zverev, A. I. Manakov, S. S. Khasanov, R. P. Shibaeva, N. D. Kushch, A. V. Kazakova, L. I. Buravov, E. B. Yagubskii, and E. Canadell, Phys. Rev. B **74**, 104504 (2006).
[15] K. Yamaji, J. Phys. Soc. Jpn. **58**, 1520 (1989).
[16] R. Yagi, Y. Iye, T. Osada, S. Kagoshima, J. Phys. Soc. Jpn. **59**, 3069 (1990).
[17] Shoenberg D. "Magnetic oscillations in metals", Cambridge University Press 1984.
[18] P.D. Grigoriev, M.V. Kartsovnik, W. Biberacher, N.D. Kushch, P. Wyder, Phys. Rev. B **65**, 60403(R) (2002).
[19] P.D. Grigoriev, M.V. Kartsovnik, W. Biberacher, P. Wyder, cond-mat/0108352 (2001) [unpublished].
[20] P.D. Grigoriev, Phys. Rev. B **67**, 144401 (2003).
[21] M.V. Kartsovnik, P.D. Grigoriev, W. Biberacher, N.D. Kushch, P. Wyder, Phys. Rev. Lett. **89**, 126802 (2002).
[22] T. Champel and V. P. Mineev, Phys. Rev. B **66**, 195111 (2002).
[23] V. M. Gvozdikov, Phys. Rev. B **70**, 085113 (2004).
[24] T. Champel and V. P. Mineev, Phys. Rev. B **74**, 247101 (2006).
[25] Tsunea Ando, J. Phys. Soc. Jpn. **36**, 1521 (1974).
[26] Tsunea Ando, J. Phys. Soc. Jpn. **37**, 622 (1974).
[27] E.M. Baskin, L.N. Magarill, and M.V. Entin, Sov. Phys. JETP **48**, 365 (1978).
[28] E. Brezin, D.I. Gross, C. Itzykson. Nucl. Phys. B **235**, 24 (1984).
[29] The Quantum Hall Effect, Ed. by R. Prange and S. M. Girvin (Springer, New York), 1987.
[30] A.M. Dyugaev, P.D. Grigor'ev, Yu.N. Ovchinnikov, JETP Letters **78**, 148 (2003).
[31] I.S. Burmistrov, M.A. Skvortsov, JETP Lett. **78**, 156 (2003).
[32] A.A. Abrikosov, *Fundamentals of the theory of metals*, North-Holland, 1988.
[33] G. Mahan "Many-Particle Physics", 2nd ed., Plenum Press, New York, 1990
[34] "Standard Mathematical Tables and Formulae", CRC Press, (1996) (or another similar book).